

Geophysical Research Letters[®]



RESEARCH LETTER

10.1029/2024GL108195

Key Points:

- Ocean heat transport drives sea-ice variability in the central and north-eastern Barents Sea
- Atmospheric temperature drives sea-ice variability in the northern Barents-Kara Seas
- Atmospheric circulation over the Nordic Seas drives ocean heat transport, which then influences sea-ice variability

Supporting Information:

Supporting Information may be found in the online version of this article.

Correspondence to:

J. Dörr,
jakob.dorr@uib.no

Citation:

Dörr, J., Årthun, M., Docquier, D., Li, C., & Eldevik, T. (2024). Causal links between sea-ice variability in the Barents-Kara Seas and oceanic and atmospheric drivers. *Geophysical Research Letters*, 51, e2024GL108195. <https://doi.org/10.1029/2024GL108195>

Received 8 JAN 2024
Accepted 21 MAR 2024

Causal Links Between Sea-Ice Variability in the Barents-Kara Seas and Oceanic and Atmospheric Drivers

Jakob Dörr¹ , Marius Årthun¹ , David Docquier² , Camille Li¹ , and Tor Eldevik¹

¹Geophysical Institute, University of Bergen and Bjerknes Centre for Climate Research, Bergen, Norway, ²Royal Meteorological Institute of Belgium, Brussels, Belgium

Abstract The sea-ice cover in the Barents and Kara Seas (BKS) displays pronounced interannual variability. Both atmospheric and oceanic drivers have been found to influence sea-ice variability, but their relative strength and regional importance remain under debate. Here, we use the Liang-Kleeman information flow method to quantify the causal influence of oceanic and atmospheric drivers on the annual sea-ice cover in the BKS in the Community Earth System Model large ensemble and reanalysis. We find that atmospheric drivers dominate in the northern part, ocean heat transport dominates in the central and northeastern part, and local sea-surface temperature dominates in the southern part. Furthermore, the large-scale atmospheric circulation over the Nordic Seas drives ocean heat transport into the Barents Sea, which then influences sea ice. Under future sea-ice retreat, the atmospheric drivers are expected to become more important.

Plain Language Summary The sea ice in the Barents and Kara Seas (BKS) is melting due to Arctic warming, but this is overlaid by large natural variability. This variability is caused by variations in the ocean and the atmosphere, but it is not clear which is more important in which parts of the region. We use a relatively new method that allows us to quantify cause-effect relationships between sea ice and atmospheric and oceanic drivers. We find that in the north of the BKS, the atmosphere has the biggest impact, in the central and northeastern parts, it is the heat from the ocean, and in the south, it is the local sea temperature. We also find that wind patterns over the Nordic Seas affect how much oceanic heat comes into the Barents Sea, and that, in turn, affects the sea ice. Looking ahead, as the ice is expected to melt more in the future, the atmosphere is likely to become more important in driving sea ice variability in the BKS. This study helps us better understand how the ocean and atmosphere work together to influence the yearly changes in sea ice in this region.

1. Introduction

Arctic sea ice has been retreating in all seasons since the late 1970s, mainly as a result of anthropogenic greenhouse gas emissions and associated global warming (Notz & Stroeve, 2016). In winter, sea ice in the Arctic is currently retreating fastest in the Barents and Kara Seas (BKS), which are already almost ice-free in summer (Onarheim et al., 2018) and will continue to lose their winter sea-ice cover unless emissions are strongly reduced (Årthun et al., 2021). However, the externally forced retreat of sea ice in the BKS is overlaid by substantial internal variability on interannual to decadal timescales, which may have contributed substantially to the recent decline in the region (Dörr et al., 2023; England et al., 2019; Onarheim & Årthun, 2017). Internal variability is the dominant source of uncertainty in sea-ice projections in the Barents Sea over the next 30 years (Bonan et al., 2021), and it is therefore important to understand the underlying drivers.

Oceanic and atmospheric processes both drive sea-ice variability in the BKS, but their relative contributions remain under debate. Variable ocean heat transport toward the Arctic, mainly through the Barents Sea Opening (BSO) (Figure 1) and to a lesser extent through Fram Strait, has been found to influence sea-ice variability in the BKS on seasonal to decadal timescales (Årthun et al., 2012, 2019; Docquier & Königk, 2021; Dörr et al., 2021; Lien et al., 2017; Nakanowatari et al., 2014; Oldenburg et al., 2023; Sandø et al., 2014; Yeager et al., 2015). On the other hand, studies also find that atmospheric variability dominates interannual sea-ice variability in the BKS through the advection of warm air and enhancement of downward long-wave radiative fluxes, and that ocean heat transport plays a smaller role on interannual timescales (Kim et al., 2019; Liu et al., 2022; Olonscheck et al., 2019; Sorokina et al., 2016; Woods & Caballero, 2016; Zheng et al., 2022).

© 2024. The Authors.

This is an open access article under the terms of the [Creative Commons Attribution License](https://creativecommons.org/licenses/by/4.0/), which permits use, distribution and reproduction in any medium, provided the original work is properly cited.

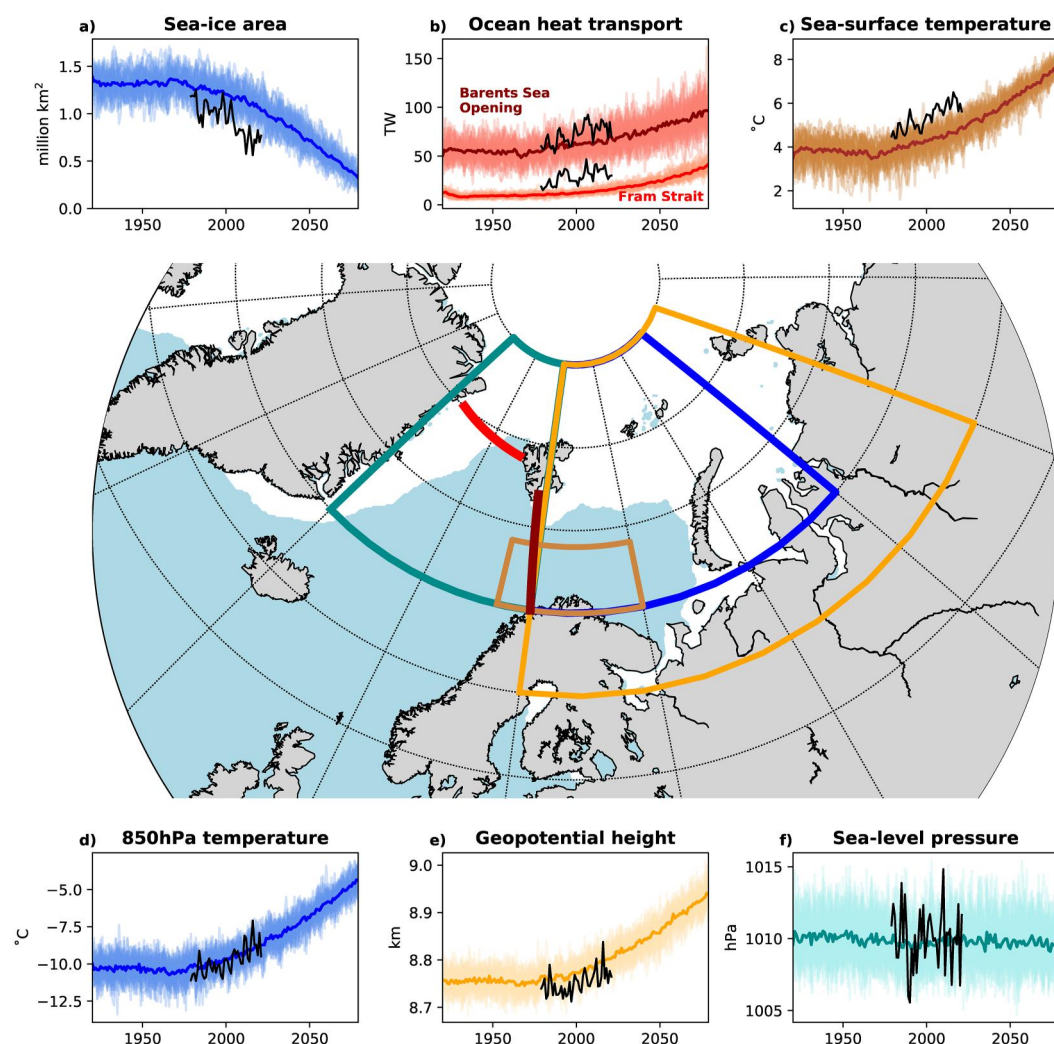


Figure 1. Potential drivers of sea-ice variability Barents-Kara Seas (BKS). (a) Sea-ice area averaged over the BKS (blue area; 20–80°E, 70–85°N), (b) ocean heat transport through the Fram Strait (red line) and Barents Sea Opening (dark red line), (c) sea-surface temperature averaged over the southwestern Barents Sea (brown area; 15–40°E, 70–74°N), (d) 850 hPa temperature averaged over the BKS, (e) 300 hPa geopotential height averaged over the extended BKS (orange area; 20–100°E, 65–85°N), and (f) sea-level pressure averaged over the Nordic Seas (dark cyan area; 20–20°E, 70–85°N). Colored lines and shading show the ensemble mean and all individual members, respectively. Black lines show data from ERA5/ORAS5 reanalysis. White/blue shading on the map shows the annual mean sea-ice cover (based on 15% sea-ice concentration) in ORAS5 over 1979–2021.

Common to most studies about oceanic or atmospheric drivers of sea-ice variability is the use of (lagged) anomaly correlations to infer causal mechanisms. Correlation in itself, however, does not imply causality. To identify cause and effect, causal inference frameworks can be used (examples of climate applications include Deza et al., 2015; Kretschmer et al., 2016; Rehder et al., 2020; Vannitsem & Eklemans, 2018). One such framework, the Liang-Kleeman information flow (Liang, 2021; Liang & Kleeman, 2005), is particularly interesting because it can quantify the direction and magnitude of causal relationships. It has been used to determine causal drivers of variability in global mean temperature (Stips et al., 2016), Antarctic ice sheet surface mass balance (Vannitsem et al., 2019), and pan-Arctic sea-ice area (SIA) (Docquier et al., 2022). Docquier et al. (2022) identified air temperature, sea surface temperature, and ocean heat transport as important drivers of sea ice variability, but did not consider the spatially non-uniform character of sea ice changes and their drivers, potentially mixing signals from different regions in the Arctic. Considering spatial differences in the drivers of sea-ice variability is especially important in the BKS because of the large changes in the last decades which may lead to changes in the importance of atmospheric and oceanic drivers.

In this work, we apply the Liang-Kleeman information flow method to data from a large ensemble of climate model simulations and reanalysis products, allowing us to determine the past and future relationships between interannual variability in BKS sea-ice cover and its potential oceanic and atmospheric drivers. In Section 2, we describe the data and methodology, in Section 3, we present our results, and we then discuss our results and conclude in Section 4.

2. Materials and Methods

We focus our analysis on output from the Community Earth System Model 1 Large Ensemble (CESM-LE; Kay et al., 2015). CESM-LE has been widely used to assess Arctic sea-ice changes and is one of the best-performing large ensembles in reproducing the patterns and amplitude of sea-ice variability (Årthun et al., 2019; England et al., 2019). CESM-LE consists of 40 members, of which we analyze output from 1920 to 2079, simulated using the historical scenario before 2005 and the high emission scenario RCP8.5 (Riahi et al., 2011) after 2005. To assess changes in causal relationships, we split the period into two 80-year sub-periods (1920–1999 and 2000–2079). The large number of ensemble members ensures a robust analysis of causal drivers. Before the analysis, we remove the ensemble mean (i.e., the forced signal) from each member, such that we only analyze internal variability. Additionally, we analyze causal relationships in reanalysis data from 1979 to 2021, using ERA5 atmospheric reanalysis (Hersbach et al., 2020; 850 hPa air temperature, 300 hPa geopotential height, sea-level pressure) and ORAS5 ocean reanalysis (Zuo et al., 2019; sea-ice concentration, ocean velocity and temperature, sea-surface temperature). ORAS5 shows skill in reproducing observed variability and trends in temperatures in the BKS (Li et al., 2022; Polyakov et al., 2023; Shu et al., 2021). We note that the results based on this relatively short single realization will be less robust than those from CESM-LE. To remove the forced signal in reanalysis data, we detrend the data using a linear fit. The forced response is likely not linear over time, and removing a linear fit is thus not the perfect way of isolating internal variability. Nevertheless, our results remain similar if we instead remove a second-order polynomial fit (not shown).

To represent the sea-ice cover in the BKS, we calculate the SIA in the region, multiplying the sea-ice concentration with the grid cell area and summing up over all grid cells in the region (Figure 1a). The drivers analyzed herein were chosen based on the literature on the atmospheric and oceanic influences on Arctic and BKS sea ice: ocean heat transport through the BSO (Årthun et al., 2012) and the northward ocean heat transport in the Fram Strait (Figure 1b), sea-surface temperature over the southwestern Barents Sea (SST_{AW} , Figure 1c; Sandø et al., 2014), air temperature at 850 hPa (T850, Figure 1d; Liu et al., 2022; Olonscheck et al., 2019; Schlichtholz, 2011), the 300 hPa geopotential height over the extended BKS (Figure 1e; Liu et al., 2022), and the sea-level pressure over the northern Nordic Seas (Figure 1f; Dörr et al., 2021; Rieke et al., 2023). We compute the ocean heat transport on the original grids of CESM and ORAS5 through the sections shown in Figure 1, using a reference temperature of 0°C, following Dörr et al. (2021). We compute annual means for all variables, to focus on interannual variability. CESM-LE shows trends similar to the reanalysis in all variables (Figure 1), but simulates a lower sea-surface temperature and ocean heat transport, and more sea ice.

We use the atmospheric temperature above the boundary layer (T850) since it is less directly tied to sea ice than surface temperatures (Olonscheck et al., 2019; Pavelsky et al., 2011), and, hence, better captures the dynamical link between atmospheric variability and variability in sea ice. The influence of atmospheric temperature on sea ice occurs mostly through changes in the surface turbulent heat (latent and sensible) and long-wave radiative fluxes (Kim et al., 2019; Liu et al., 2022; Sorokina et al., 2016; Woods & Caballero, 2016). Since our analysis is based on annual means and spatial averages over areas with seasonal ice cover, it will integrate flux anomalies that both drive and are driven by sea-ice anomalies. We, therefore, do not include surface fluxes as a potential driver of sea-ice variability. Thermodynamic forcing through anomalous downwelling longwave radiative flux at the surface, which is suggested to be a main atmospheric driver of sea ice variability, is related to anticyclonic anomalies over the eastern BKS (Liu et al., 2022) and is captured by the geopotential height index.

To reveal the causal relationships between BKS sea ice and its potential drivers, we use the Liang-Kleeman information flow method (Liang, 2021; Liang & Kleeman, 2005). The method computes the absolute rate of information transfer from variable X_j to variable X_i as

$$T_{j \rightarrow i} = \frac{1}{\det \mathbf{C}} \cdot \sum_{k=1}^N \Delta_{jk} C_{k,di} \cdot \frac{C_{ij}}{C_{ii}} \quad (1)$$

where \mathbf{C} is the covariance matrix, N is the number of variables (seven in our case; SIA and six potential drivers), Δ_{jk} are the cofactors of \mathbf{C} , $C_{k,di}$ is the sample covariance between X_k and the Euler forward difference in time of X_i , C_{ij} is the sample covariance between X_i and X_j and C_{ii} is the sample variance of X_i . When X_j has a causal influence on X_i , $T_{j \rightarrow i}$ is significantly different from zero, whereas when there is no influence, $T_{j \rightarrow i}$ is zero. We compute statistical significance using bootstrap resampling with replacement of all terms in Equation 1 using 1000 realizations. We further normalize the rate of information transfer and express it in percent, as the absolute value of the relative rate of information transfer $|\tau_{j \rightarrow i}|$ (see Liang (2021) for more details). A value of $|\tau_{j \rightarrow i}|$ of 100% means a maximum influence, while 0% means no influence. Note that the percentage cannot be quantitatively interpreted as an explained variance, however, values can be compared to determine which variables have the largest influence.

We apply the Liang-Kleeman information flow method to the BKS SIA and the six potential drivers mentioned above. For CESM-LE, we follow Docquier et al. (2022) and compute $|\tau|$ for each member's detrended data (ensemble mean removed) and then compute the mean across ensemble members. Statistical significance is calculated using Fisher's method for multiple tests (Fisher, 1992). Furthermore, to analyze spatial differences in the causal relationships between BKS sea ice and its drivers, we repeat the analysis for each grid point in the BKS and replace the total SIA with the annual mean sea-ice concentration at this grid point. We then obtain spatial maps of the relative rate of information transfer between local sea-ice concentration and the same regional drivers mentioned above. We calculate significance for each grid point in the same way as for the SIA, but we additionally apply a False Discovery Rate (FDR; Docquier et al., 2023; Wilks, 2016) to account for the multiplicity of tests.

3. Results

3.1. Causal Links in CESM-LE

We first assess the causal relationships between the BKS SIA and its potential drivers in CESM-LE for the two different periods, 1920–1999 and 2000–2079. Figure 2 shows matrices of the relative rates of information transfer and correlation coefficients between sea ice and all its potential drivers, averaged over all CESM-LE members. In both periods, the self-influence (diagonal) shows the highest $|\tau|$, ranging from 29% to 62%. Self-influence can be interpreted as the influence of the variable state on the dynamics of the variable itself (Docquier et al., 2022; Liang, 2021).

As for the causal influence between sea ice and the other variables, the heat transport through the BSO has the largest influence on SIA in the BKS during the two periods ($|\tau| = 10\%$ in 1920–1999 and 6% in 2000–2079; Figures 2a and 2c), despite not being the variable with the highest correlation ($R = -0.63$ in 1920–1999 and -0.45 in 2000–2079; Figures 2b and 2d). The second variable having a significant influence on sea ice is T850 ($|\tau| = 4\%$ in 1920–1999 and 7% in 2000–2079). SST_{AW} is highly correlated to the SIA ($R = -0.81$ in 1920–1999 and -0.69 in 2000–2079) but does not have a significant causal influence on sea ice in either period. This shows the usefulness of the causal analysis, as it identifies actual causal links rather than simple correlations between variables. Despite being significantly correlated with the SIA, the influence of the atmospheric circulation indices (geopotential height and sea-level pressure) on the sea ice is not significant.

Besides influencing the SIA, the heat transport through the BSO also influences SST_{AW} in both periods (fourth row in Figures 2a and 2c). This underscores the importance of the oceanic heat imported into the Barents Sea in setting the ocean temperatures and ice cover (Årthun et al., 2012). Furthermore, CESM-LE shows a significant correlation between the heat transport through Fram Strait and the BSO in the first period ($R = 0.49$), which is likely due to similar atmospheric influence (Dörr et al., 2021). The information flow method picks up this connection as an influence from the BSO to the Fram Strait ($|\tau| = 10\%$), which is expected since the BSO is upstream of the Fram Strait. Finally, the variability in BSO heat transport is significantly influenced by sea-level pressure over the Nordic Seas during the first period ($|\tau| = 5\%$), confirming that interannual variability of ocean heat transport is driven by atmospheric circulation (Brown et al., 2023; Dörr et al., 2021; Madonna &

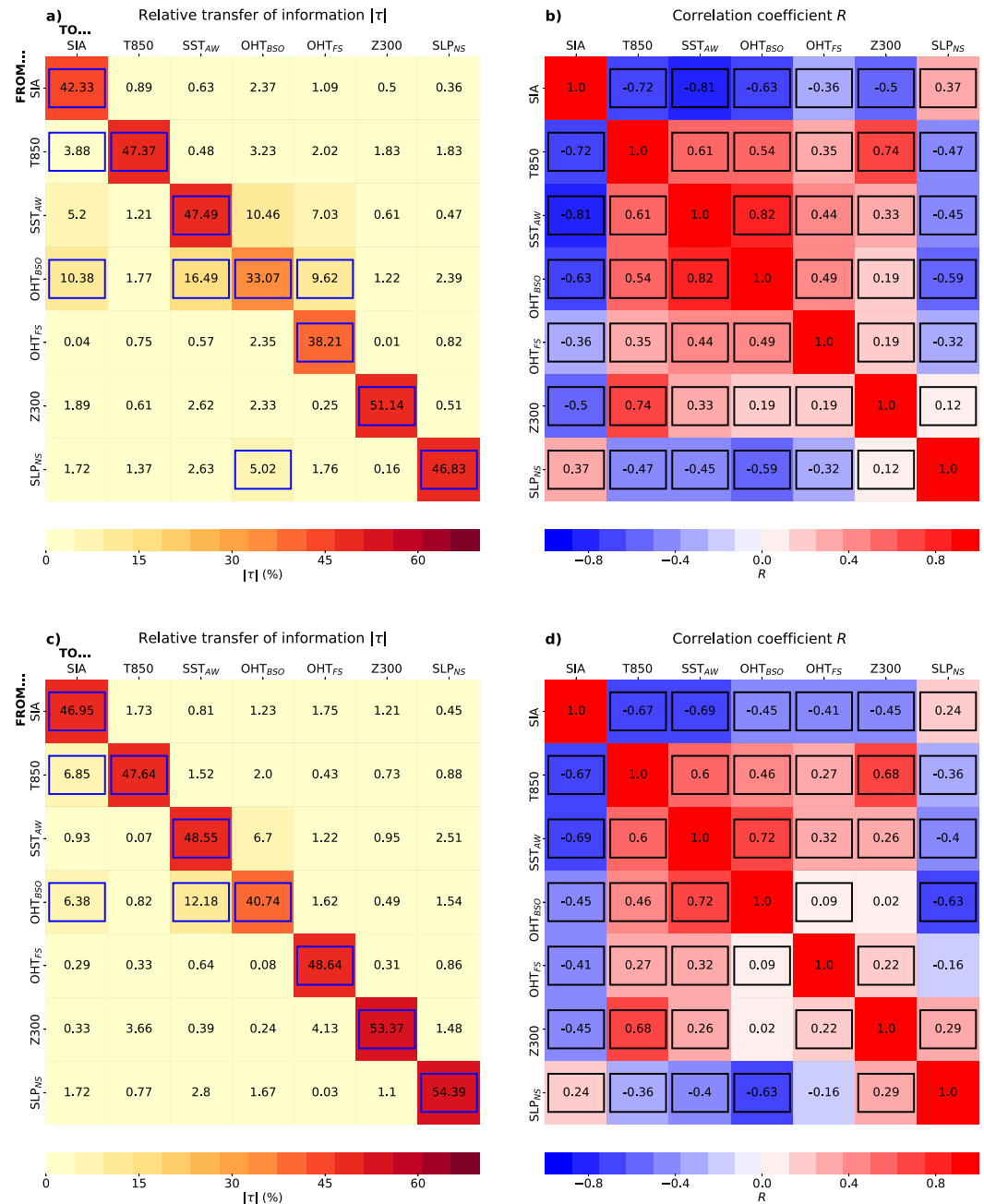


Figure 2. Causal drivers of sea ice variability in the Barents-Kara Seas (BKS). Matrix with relative rates of information transfer (a, c) and correlation coefficients (b, d) between each variable in the BKS for 1920–1999 (a, b) and 2000–2079 (c, d) averaged over 40 members from CESM-LE. Variables include the sea-ice area (SIA) over the BKS (SIA), the 850 hPa air temperature (T850), the sea-surface temperature over the southwestern Barents Sea (SST_{AW}), the ocean heat transport through the Barents Sea Opening (OHT_{BSO}), the ocean heat transport through the Fram Strait (OHT_{FS}), the 300-hPa geopotential over the extended region (Z300), and the sea-level pressure over the Nordic Seas (SLP_{NS}). The highlighted elements are significant at the 5% confidence level based on Fisher's method for multiple tests.

Sandø, 2022; Muilwijk et al., 2019). These results suggest that for annual means, the direct influence of the large-scale atmospheric circulation on sea ice in the BKS is weak, but a causal chain exists whereby the Nordic sea-level pressure influences the oceanic heat transport into the BKS, which then influences sea ice.

In the second period, as the sea ice retreats northward, the influence of the BSO heat transport on sea ice becomes weaker ($|\tau| = 6\%$, Figure 2c). On the other hand, the influence of T850 becomes larger ($|\tau| = 7\%$), indicating that

atmospheric temperatures will be increasingly important for sea-ice variability in the future BKS. The influence of sea-level pressure over the Nordic Seas on the BSO heat transport weakens and is no longer significant in the second period, while their correlation stays high. We note that when we expand the area over which we average the sea-level pressure to the south, its influence is still significant in both periods (not shown), indicating that the large-scale influence of the atmospheric circulation over the Nordic Seas remains an important driver of ocean heat transport into the Barents Sea.

We next look at the spatial distribution of the causal relationships between sea ice and its potential drivers in CESM-LE by replacing the BKS SIA with the local sea ice concentration and repeating the analysis for every grid point in the BKS. We show the causal relationship in both directions for sea ice and the BSO heat transport, T_{850} , SST_{AW} , and the geopotential height index for the second period in Figure 3. We choose to show the second period only (2000–2079) because it is the period where the average SIA is closer to the reanalysis data (Figure 1). We show the interaction of sea ice with all variables during both periods in Figures S1 and S2 in Supporting Information S1.

The causal method reveals that atmospheric temperatures (T_{850}) mainly influence sea ice in the northern and eastern BKS, while sea-surface temperatures in the southern Barents Sea (SST_{AW}) mainly influence sea ice in the central and southern Barents Sea (Figures 3a and 3b left). The regions of significant influence are broadly consistent with the regions of maximum correlation (right column in Figures 3a and 3b), although the correlations are significant in the entire BKS region for both variables. The local influence of the BSO heat transport on sea ice is significant in the northeastern Barents Sea, approximately in between the influence regions of T_{850} and SST_{AW} (Figure 3c). However, unlike the correlation, which also shows a maximum in the southern BKS, $|r|$ is not significant there, indicating no direct influence of the BSO heat transport on sea ice in this region. The results show a similar tripartition in the earlier period (Figure S2 in Supporting Information S1). However, the influence of SST and T_{850} is more limited, and the influence of the BSO ocean heat transport is strong across the entire Barents Sea, which confirms results obtained with SIA instead of sea ice concentration (Figure 2).

The atmospheric geopotential height index (Z_{300}) is well correlated with the sea ice concentration in the northern BKS (as also shown in Liu et al. (2022)). The significant influence on sea ice is, however, restricted to the area south of Svalbard in the first period (Figure S2 in Supporting Information S1) and almost disappears in the second period (Figure 3e). The sea-level pressure over the Nordic Seas is well correlated to sea ice in the southern BKS, but the information flow method shows no significant influence (Figure S1 in Supporting Information S1). This corroborates the result from Figure 2 that the sea-level pressure influences sea ice in the southern Barents Sea mainly via the BSO heat transport.

In summary, we find that in CESM-LE, the BSO heat transport has the strongest influence on sea ice in the first period, mostly affecting sea ice in the central and northeastern Barents Sea. Sea ice in the northern BKS is mostly affected by atmospheric temperature, which has the strongest total influence in the second period. Sea ice in the southern Barents Sea is mostly affected by local sea-surface temperature. We further find a causal chain in which the atmosphere influences ocean heat transport into the Barents Sea, which then influences sea ice.

3.2. Causal Links in Reanalysis

To evaluate the results from CESM-LE, we briefly analyze causal relationships between BKS sea ice and its drivers in reanalysis data from 1979 to 2021. Because of the relatively short observational period, large internal variability, and only one realization, the relative transfer of information between the BKS SIA and the other variables is not significant (Figure S3 in Supporting Information S1). We therefore directly turn to the regional relationships between sea-ice concentration and T_{850} , SST_{AW} , the BSO heat transport, and the geopotential height index in Figure 4. Note that we use a significance level of 10% to account for the short observational period. Even though most values are not significant, it is still useful to compare the results with those from CESM-LE. The relationship of sea ice with all variables is shown in Figure S4 in Supporting Information S1. Like in CESM-LE, the BSO heat transport significantly influences sea ice concentration in the northern and northeastern Barents Sea, although over a smaller area than in CESM-LE, and a bit more to the west. The influence of SST_{AW} is limited in reanalysis. Similar to CESM-LE, the reanalysis data shows the largest (although not significant) influence of T_{850} in the northern BKS.

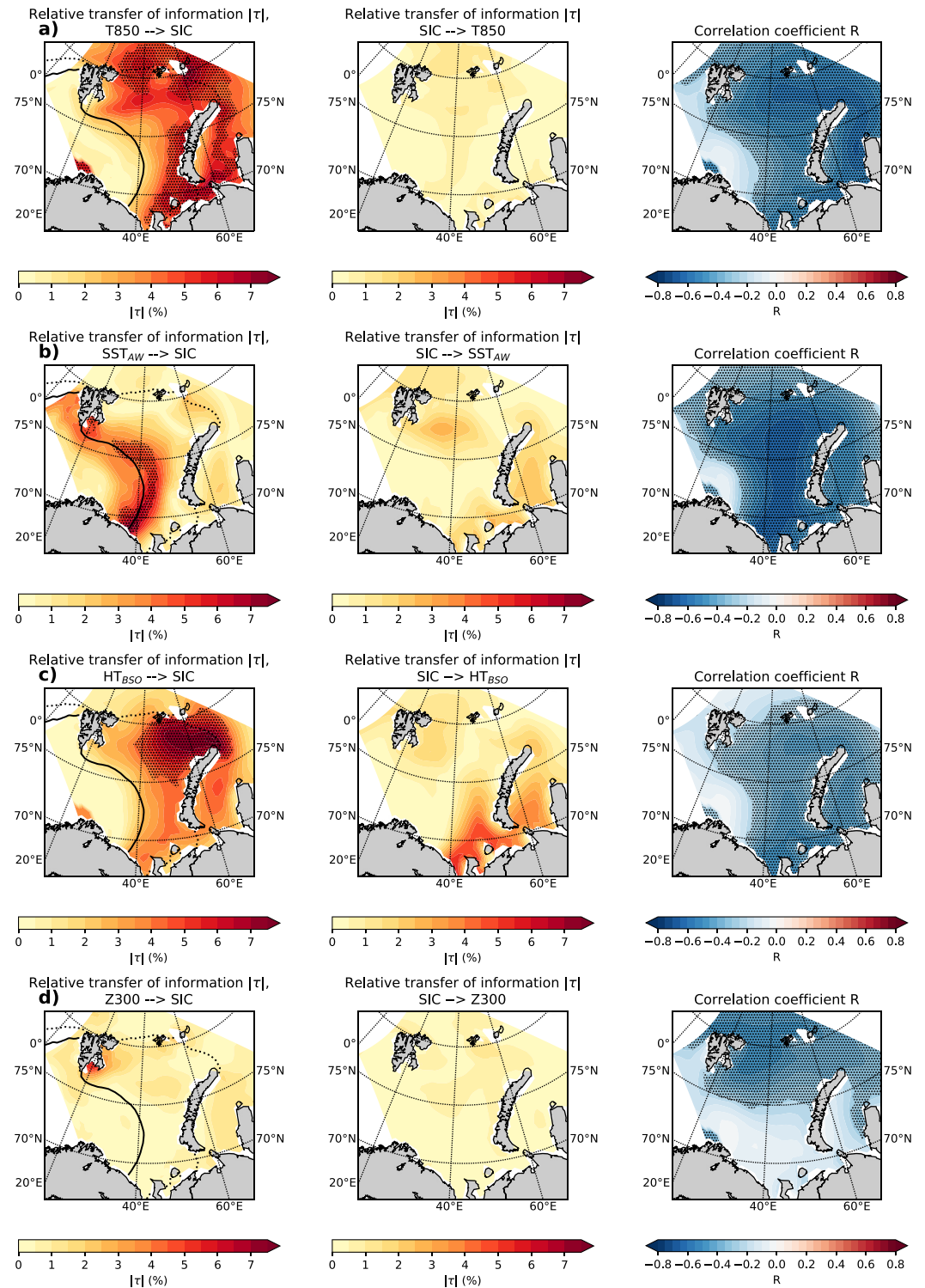


Figure 3. Regional influence on Barents-Kara Seas (BKS) sea ice. Maps of relative rates of information transfer (in the two directions) and correlation coefficients between annual mean sea-ice concentration and (a) 850 hPa temperature (T850) over the BKS, (b) sea-surface temperature (SST_{AW}) over the southwestern BKS, (c) heat transport through the Barents Sea Opening (HT_{BSO}), and (d) 300 hPa geopotential height (Z300) over the BKS, for CESM-LE over 2000–2079. The black contour line in the left panels denotes the ensemble mean sea-ice edge (based on 15% sea-ice concentration) in 2000, and the dashed line the sea-ice edge in 2079. Black stippling denotes statistically significant values (FDR 5%; 1,000 bootstrap samples).

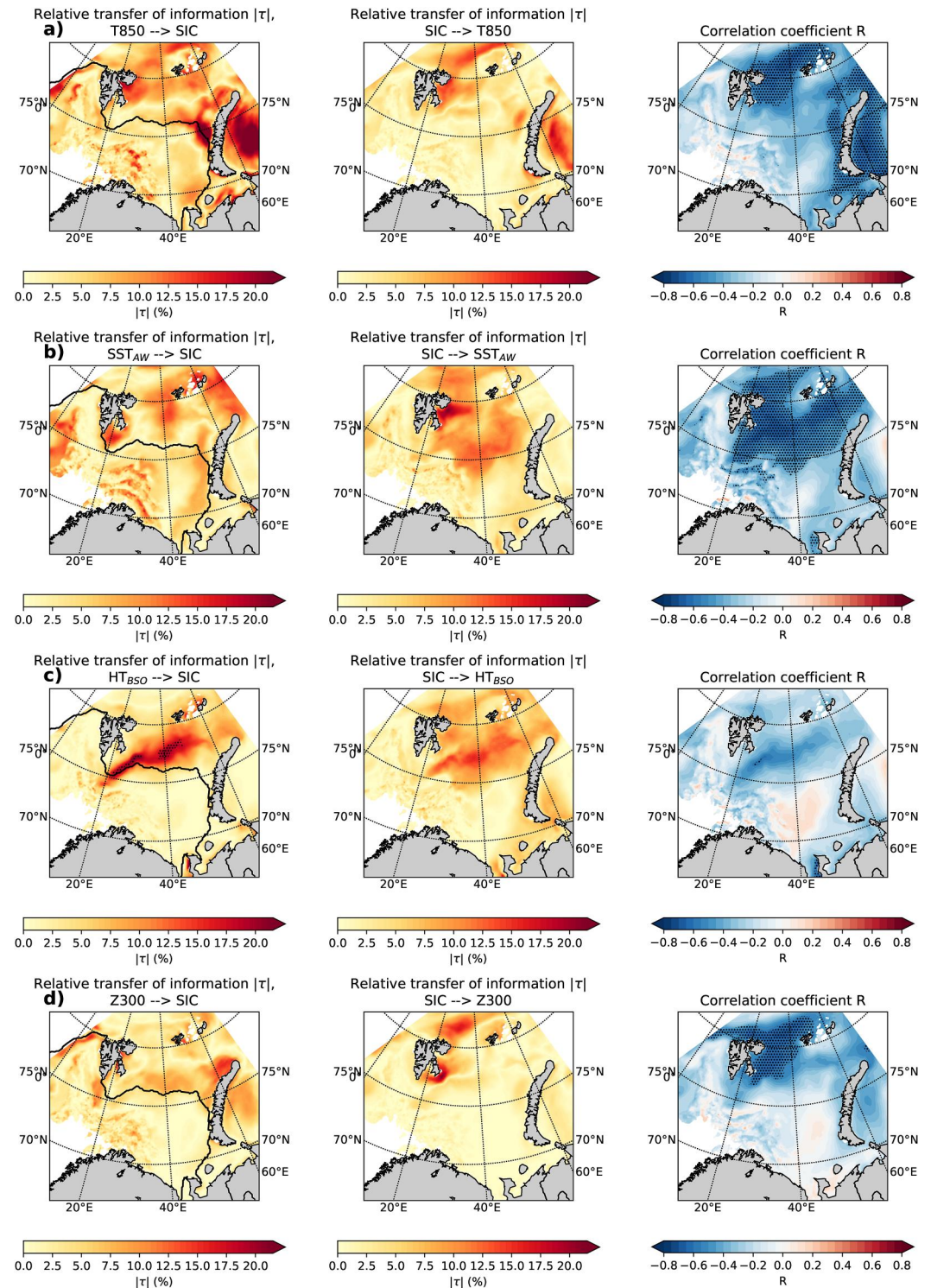


Figure 4. As Figure 3, but for ORAS5/ERA5 in 1979–2021. The black contour line in the left panels denotes the ensemble mean sea-ice edger (based on 15% sea-ice concentration) in 1979–2021. Black stippling denotes statistically significant values (FDR 10%; 1,000 bootstrap samples).

The correlation maps for sea ice and the geopotential height index (Z300) look similar to CESM-LE, with Z300 being correlated with sea-ice concentration in the northern Barents Sea (Figure 4e). This area corresponds to elevated rates of information transfer from sea ice to Z300, albeit not significant.

Although the influences are mostly not significant, the reanalysis data generally supports the partitioning of the Barents Sea ice cover into a northern part influenced by atmospheric temperatures, and a central part influenced by ocean heat transport, although the partitioning is not as clear as in CESM-LE. Furthermore, the reanalysis also supports the notion that, for annual means and on interannual timescales, the atmospheric circulation indices have little direct influence on the sea ice cover, but instead influence the ocean heat transport into the Barents Sea (Figure S3 in Supporting Information S1).

4. Discussion and Conclusions

We have used the Liang-Kleeman information flow method (Liang, 2021; Liang & Kleeman, 2005) to analyze causal relationships between annual-mean sea ice variability and its atmospheric and oceanic drivers in the BKS based on the CESM-LE large ensemble (1920–2079) and reanalysis data (1979–2021). We find that in CESM-LE, the ocean heat transport into the Barents Sea is a main driver of present and future sea ice variability, consistent with previous studies (Årthun et al., 2012; Decuyper et al., 2022; Docquier et al., 2021; Dörr et al., 2021; Rieke et al., 2023). Furthermore, we find a tripartition of the Barents-Kara sea ice, with the northern part being predominantly influenced by atmospheric temperature (Arctic domain), the southern part influenced by local sea-surface temperature (Atlantic domain), and the region between the two domains influenced by ocean heat transport. We further find that as the sea ice cover in the Barents-Kara Seas retreats in the future, the influence of sea-surface temperature and ocean heat transport decreases, while the atmospheric influence increases, as suggested by Smedsrud et al. (2013).

Previous studies have identified a strong influence of atmospheric circulation patterns on subseasonal to inter-annual sea ice variability in the BKS during the cold season, both in observations/reanalysis (Blackport et al., 2019; Deser et al., 2000; Kimura & Wakatsuchi, 2001; Siew et al., 2023; Sorokina et al., 2016) and modeling experiments (Blackport et al., 2019; Liu et al., 2022; Siew et al., 2023). On decadal and longer time scales, large-scale atmospheric circulation as well as ocean heat transport and Atlantic Water properties have been found to influence sea ice variability (Polyakov et al., 2023; Yashayaev & Seidov, 2015; Zhang, 2015). Our results focusing on annual means indicate that the direct influence of circulation patterns on Barents-Kara sea ice variability is weak and regionally confined. Rather, we show indirect influences via atmospheric temperature as well as via a causal chain where the atmospheric circulation over the Nordic Seas drives variability of ocean heat transport into the Barents Sea, which then drives sea-ice variability, consistent with Sorteberg and Kvingsdal (2006) and Mulwijk et al. (2019). These indirect influences seem reasonable given our use of annual-mean atmospheric circulation patterns, whose variability reflects more integrated signals of global climate change.

Results from reanalysis data, although mostly non-significant, generally agree with CESM-LE, but show a weaker influence of ocean heat transport (Figure S3 in Supporting Information S1). On the one hand, this is likely related to the uncertainty of using a single 43-year time series. The influence of the ocean becomes slightly stronger when using the reanalysis products back to 1958 (not shown), although there are larger uncertainties due to fewer observations and model spin-up in ORAS5 (Zuo et al., 2019). On the other hand, the difference between CESM-LE and reanalysis data could be related to biases in the CESM-LE. Even though CESM1 is among the best performing models in simulating Arctic sea-ice variability (Årthun et al., 2019; Dörr et al., 2024; England et al., 2019), it has a cold bias in the BKS (Figures 1a and 1c). This delays the sea-ice loss and the associated weakening of the oceanic influence compared to reanalysis and we would expect the oceanic influence to be stronger in CESM-LE than in reanalysis data for the recent decades, as is seen. In reality, the atmospheric influence likely begins to strengthen earlier than projected by CESM-LE.

A main novelty of our results is that they go beyond simple correlations, which do not necessarily imply causality and do not reveal the direction of possible causal relationships. That said, the correlation is still a useful diagnostic in the case of a known relationship, such as between ocean heat transport and sea ice. Furthermore, we acknowledge the limitations of using the Liang-Kleeman information flow method. First, the method is valid for linear systems and will only give an approximate solution for non-linear systems. The method has, however, been validated using highly non-linear synthetic examples (Liang, 2021), and has been successfully used to detect causal influences in the climate system (Docquier et al., 2022; Liang, 2014; Stips et al., 2016). Non-linear estimates of the rate of information transfer (e.g., Pires et al., 2023) have therefore not been applied here. Second, there might be hidden variables that have an influence on sea ice in the Barents-Kara Seas but that are not included here. However, we have carefully checked the literature to account for all relevant variables, so the effect of

hidden variables is likely limited. Despite these two limitations, this causal method provides highly valuable information on causal drivers of annual sea ice variability in the BKS beyond correlation and regression analyses.

Data Availability Statement

All data in this study are publicly available. Output from ORAS5 is available through the Copernicus Climate Change Service's Climate Data Store (Copernicus Climate Change Service, 2021). Output from ERA5 is available through the Copernicus Climate Change Service's Climate Data Store (Copernicus Climate Change Service, 2019a, 2019b). Output from CESM-LE is available via the Earth System Grid (Climate Data Gateway, 2021). Python functions used to calculate the Liang-Kleeman information flow as in Docquier et al. (2022) can be downloaded from https://github.com/Climdyn/Liang_Index_climdyn.

Acknowledgments

This study was funded by the Research Council of Norway projects Nansen Legacy (Grant 276730) and the Trond Mohn Foundation (Grant BFS2018TMT01). David Docquier is funded by the Belgian Science Policy Office (BELSPO) under the RESIST project (contract no. RT/23/RESIST). Camille Li is funded by the Research Council of Norway Grant 325440. We thank the CESM Large Ensemble Community Project for making their data publicly accessible. The results contain modified Copernicus Climate Change Service information 2023. Neither the European Commission nor ECMWF is responsible for any use that may be made of the Copernicus information or data it contains. We thank two anonymous reviewers for constructive comments that helped to improve the manuscript.

References

- Årthun, M., Eldevik, T., & Smedsrud, L. H. (2019). The role of Atlantic heat transport in future Arctic winter Sea Ice loss. *Journal of Climate*, 32(11), 3327–3341. <https://doi.org/10.1175/JCLI-D-18-0750.1>
- Årthun, M., Eldevik, T., Smedsrud, L. H., Skagseth, Ø., & Ingvaldsen, R. B. (2012). Quantifying the influence of Atlantic heat on Barents Sea Ice variability and retreat. *Journal of Climate*, 25(13), 4736–4743. <https://doi.org/10.1175/JCLI-D-11-00466.1>
- Årthun, M., Onarheim, I. H., Dörr, J., & Eldevik, T. (2021). The seasonal and regional transition to an ice-free Arctic. *Geophysical Research Letters*, 48(1), e2020GL090825. <https://doi.org/10.1029/2020GL090825>
- Blackport, R., Screen, J. A., van der Wiel, K., & Bintanja, R. (2019). Minimal influence of reduced Arctic sea ice on coincident cold winters in mid-latitudes. *Nature Climate Change*, 9(9), 697–704. <https://doi.org/10.1038/s41558-019-0551-4>
- Bonan, D. B., Lehner, F., & Holland, M. M. (2021). Partitioning uncertainty in projections of Arctic sea ice. *Environmental Research Letters*, 16(4), 044002. <https://doi.org/10.1088/1748-9326/abe0ec>
- Brown, N. J., Mauritzen, C., Li, C., Madonna, E., Isachsen, P. E., & LaCasce, J. H. (2023). Rapid response of the Norwegian Atlantic slope current to wind forcing. *Journal of Physical Oceanography*, 53(2), 389–408. <https://doi.org/10.1175/JPO-D-22-0014.1>
- Climate Data Gateway. (2021). Dataset: CESM1 large ensemble [Dataset]. *Climate Data Gateway*. Retrieved from <https://www.earthsystemgrid.org/dataset/ucar.cgd.cesm4.cesmLE.html>
- Copernicus Climate Change Service. (2019a). ERA5 monthly averaged data on pressure levels from 1979 to present. *ECMWF*. <https://doi.org/10.24381/CD5.6860A573>
- Copernicus Climate Change Service. (2019b). ERA5 monthly averaged data on single levels from 1979 to present. *ECMWF*. <https://doi.org/10.24381/CD5.F17050D7>
- Copernicus Climate Change Service. (2021). ORAS5 global ocean reanalysis monthly data from 1958 to present. *ECMWF*. <https://doi.org/10.24381/CD5.67E8EEB7>
- Decuyppère, M., Tremblay, L. B., & Dufour, C. O. (2022). Impact of Ocean Heat transport on Arctic Sea Ice variability in the GFDL CM2-O model suite. *Journal of Geophysical Research: Oceans*, 127(3), e2021JC017762. <https://doi.org/10.1029/2021JC017762>
- Deser, C., Walsh, J. E., & Timlin, M. S. (2000). Arctic sea ice variability in the context of recent atmospheric circulation trends. *Journal of Climate*, 13(3), 617–633. [https://doi.org/10.1175/1520-0442\(2000\)013<0617:ASIVTY>2.0.CO;2](https://doi.org/10.1175/1520-0442(2000)013<0617:ASIVTY>2.0.CO;2)
- Deza, J. I., Barreiro, M., & Masoller, C. (2015). Assessing the direction of climate interactions by means of complex networks and information theoretic tools. *Chaos*, 25(3), 033105. <https://doi.org/10.1063/1.4914101>
- Docquier, D., Koenig, T., Fuentes-Franco, R., Karami, M. P., & Ruprich-Robert, Y. (2021). Impact of ocean heat transport on the Arctic sea-ice decline: A model study with EC-Earth3. *Climate Dynamics*, 56(5), 1407–1432. <https://doi.org/10.1007/s00382-020-05540-8>
- Docquier, D., & König, T. (2021). A review of interactions between ocean heat transport and Arctic sea ice. *Environmental Research Letters*, 16(12), 123002. <https://doi.org/10.1088/1748-9326/ac30be>
- Docquier, D., Vannitsem, S., & Bellucci, A. (2023). The rate of information transfer as a measure of ocean–atmosphere interactions. *Earth System Dynamics*, 14(3), 577–591. <https://doi.org/10.5194/esd-14-577-2023>
- Docquier, D., Vannitsem, S., Ragone, F., Wyser, K., & Liang, X. S. (2022). Causal links between Arctic Sea Ice and its potential drivers based on the rate of information transfer. *Geophysical Research Letters*, 49(9), e2021GL095892. <https://doi.org/10.1029/2021GL095892>
- Dörr, J. S., Årthun, M., Eldevik, T., & Madonna, E. (2021). Mechanisms of regional winter Sea-Ice variability in a warming Arctic. *Journal of Climate*, 34(21), 8635–8653. <https://doi.org/10.1175/JCLI-D-21-0149.1>
- Dörr, J. S., Årthun, M., Eldevik, T., & Sandø, A. B. (2024). Expanding influence of Atlantic and Pacific Ocean heat transport on winter sea-ice variability in a warming Arctic. *Journal of Geophysical Research: Oceans*, 129(2), e2023JC019900. <https://doi.org/10.1029/2023JC019900>
- Dörr, J. S., Bonan, D. B., Årthun, M., Svendsen, L., & Wills, R. C. J. (2023). Forced and internal components of observed Arctic sea-ice changes. In *The cryosphere discussions* (pp. 1–27). <https://doi.org/10.5194/cr-2023-29>
- England, M., Jahn, A., & Polvani, L. (2019). Nonuniform contribution of internal variability to recent Arctic Sea Ice loss. *Journal of Climate*, 32(13), 4039–4053. <https://doi.org/10.1175/JCLI-D-18-0864.1>
- Fisher, R. A. (1992). Statistical methods for Research workers. In S. Kotz & N. L. Johnson (Eds.), *Breakthroughs in statistics: Methodology and distribution* (pp. 66–70). Springer. https://doi.org/10.1007/978-1-4612-4380-9_6
- Hersbach, H., Bell, B., Berrisford, P., Hirahara, S., Horányi, A., Muñoz-Sabater, J., et al. (2020). The ERA5 global reanalysis. *The Quarterly Journal of the Royal Meteorological Society*, 146(730), 1999–2049. <https://doi.org/10.1002/qj.3803>
- Kay, J. E., Deser, C., Phillips, A., Mai, A., Hannay, C., Strand, G., et al. (2015). The community Earth system model (CESM) large ensemble project: A community resource for studying climate change in the presence of internal climate variability. *Bulletin American Meteorology Society*, 96(8), 1333–1349. <https://doi.org/10.1175/BAMS-D-13-00255.1>
- Kim, K.-Y., Kim, J.-Y., Kim, J., Yeo, S., Na, H., Hamlington, B. D., & Leben, R. R. (2019). Vertical feedback mechanism of winter arctic amplification and Sea Ice loss. *Scientific Reports*, 9(1), 1184. <https://doi.org/10.1038/s41598-018-38109-x>
- Kimura, N., & Wakatsuchi, M. (2001). Mechanisms for the variation of sea ice extent in the northern hemisphere. *Journal of Geophysical Research*, 106(C12), 31319–31331. <https://doi.org/10.1029/2000JC000739>

- Kretschmer, M., Coumou, D., Donges, J. F., & Runge, J. (2016). Using causal effect networks to analyze different Arctic drivers of midlatitude winter circulation. *Journal of Climate*, 29(11), 4069–4081. <https://doi.org/10.1175/JCLI-D-15-0654.1>
- Li, Z., Ding, Q., Steele, M., & Schweiger, A. (2022). Recent upper Arctic Ocean warming expedited by summertime atmospheric processes. *Nature Communications*, 13(1), 362. <https://doi.org/10.1038/s41467-022-28047-8>
- Liang, X. S. (2014). Unraveling the cause-effect relation between time series. *Physical Review E*, 90(5), 052150. <https://doi.org/10.1103/PhysRevE.90.052150>
- Liang, X. S. (2021). Normalized multivariate time series causality analysis and causal graph reconstruction. *Entropy*, 23(6), 679. <https://doi.org/10.3390/e23060679>
- Liang, X. S., & Kleeman, R. (2005). Information transfer between dynamical system components. *Physical Review Letters*, 95(24), 244101. <https://doi.org/10.1103/PhysRevLett.95.244101>
- Lien, V. S., Schlichtholz, P., Skagseth, Ø., & Vikebø, F. B. (2017). Wind-driven Atlantic water flow as a direct mode for reduced Barents Sea Ice cover. *Journal of Climate*, 30(2), 803–812. <https://doi.org/10.1175/JCLI-D-16-0025.1>
- Liu, Z., Risi, C., Codron, F., Jian, Z., Wei, Z., He, X., et al. (2022). Atmospheric forcing dominates winter Barents-Kara sea ice variability on interannual to decadal time scales. *Proceedings of the National Academy of Sciences*, 119(36), e2120770119. <https://doi.org/10.1073/pnas.2120770119>
- Madonna, E., & Sandø, A. B. (2022). Understanding differences in north Atlantic poleward Ocean Heat transport and its variability in global climate models. *Geophysical Research Letters*, 49(1), e2021GL096683. <https://doi.org/10.1029/2021GL096683>
- Muiliwijk, M., Ilicak, M., Cornish, S. B., Danilov, S., Gelderloos, R., Gerdes, R., et al. (2019). Arctic Ocean response to Greenland sea wind anomalies in a suite of model simulations. *Journal of Geophysical Research: Oceans*, 124(8), 6286–6322. <https://doi.org/10.1029/2019JC015101>
- Nakanowatari, T., Sato, K., & Inoue, J. (2014). Predictability of the Barents Sea Ice in early winter: Remote effects of oceanic and atmospheric thermal conditions from the north Atlantic. *Journal of Climate*, 27(23), 8884–8901. <https://doi.org/10.1175/JCLI-D-14-00125.1>
- Notz, D., & Stroeve, J. (2016). Observed Arctic sea-ice loss directly follows anthropogenic CO₂ emission. *Science*, 354(6313), 747–750. <https://doi.org/10.1126/science.aag2345>
- Oldenburg, D., Kwon, Y.-O., Frankignoul, C., Danabasoglu, G., Yeager, S., & Kim, W. M. (2023). The respective roles of ocean heat transport and surface heat fluxes in driving Arctic Ocean warming and sea-ice decline. *Journal of Climate*, 37(4), 1431–1448. <https://doi.org/10.1175/JCLI-D-23-0399.1>
- Olonscheck, D., Mauritsen, T., & Notz, D. (2019). Arctic sea-ice variability is primarily driven by atmospheric temperature fluctuations. *Nature Geoscience*, 12(6), 430–434. <https://doi.org/10.1038/s41561-019-0363-1>
- Onarheim, I. H., & Årthun, M. (2017). Toward an ice-free Barents Sea. *Geophysical Research Letters*, 44(16), 8387–8395. <https://doi.org/10.1002/2017GL074304>
- Onarheim, I. H., Eldevik, T., Smedsrud, L. H., & Stroeve, J. C. (2018). Seasonal and regional manifestation of Arctic Sea Ice loss. *Journal of Climate*, 31(12), 4917–4932. <https://doi.org/10.1175/JCLI-D-17-0427.1>
- Pavelsky, T. M., Boë, J., Hall, A., & Fetzer, E. J. (2011). Atmospheric inversion strength over polar oceans in winter regulated by sea ice. *Climate Dynamics*, 36(5), 945–955. <https://doi.org/10.1007/s00382-010-0756-8>
- Pires, C. A., Docquier, D., & Vannitsem, S. (2023). A general theory to estimate Information transfer in nonlinear systems. *Physica D: Nonlinear Phenomena*, 133988, 133988. <https://doi.org/10.1016/j.physd.2023.133988>
- Polyakov, I. V., Ingvaldsen, R. B., Pnyushkov, A. V., Bhatt, U. S., Francis, J. A., Janout, M., et al. (2023). Fluctuating Atlantic inflows modulate Arctic atlantification. *Science*, 381(6661), 972–979. <https://doi.org/10.1126/science.adh5158>
- Rehder, Z., Niederrenk, A. L., Kaleschke, L., & Kutzbach, L. (2020). Analyzing links between simulated Laptev Sea sea ice and atmospheric conditions over adjoining landmasses using causal-effect networks. *The Cryosphere*, 14(11), 4201–4215. <https://doi.org/10.5194/tc-14-4201-2020>
- Riahi, K., Rao, S., Krey, V., Cho, C., Chirkov, V., Fischer, G., et al. (2011). RCP 8.5—A scenario of comparatively high greenhouse gas emissions. *Climatic Change*, 109(1), 33–57. <https://doi.org/10.1007/s10584-011-0149-y>
- Rieke, O., Årthun, M., & Dörr, J. S. (2023). Rapid sea ice changes in the future Barents Sea. *The Cryosphere*, 17(4), 1445–1456. <https://doi.org/10.5194/tc-17-1445-2023>
- Sandø, A. B., Gao, Y., & Langehaug, H. R. (2014). Poleward ocean heat transports, sea ice processes, and Arctic sea ice variability in NorESM1-M simulations. *Journal of Geophysical Research: Oceans*, 119(3), 2095–2108. <https://doi.org/10.1002/2013JC009435>
- Schlichtholz, P. (2011). Influence of oceanic heat variability on sea ice anomalies in the Nordic Seas. *Geophysical Research Letters*, 38(5), L05705. <https://doi.org/10.1029/2010GL045894>
- Shu, Q., Wang, Q., Song, Z., & Qiao, F. (2021). The poleward enhanced Arctic Ocean cooling machine in a warming climate. *Nature Communications*, 12(1), 2966. <https://doi.org/10.1038/s41467-021-23321-7>
- Siew, P. Y. F., Wu, Y., Ting, M., Zheng, C., Clancy, R., Kurtz, N. T., & Seager, R. (2023). Physical links from atmospheric circulation patterns to Barents-Kara sea ice variability from synoptic to seasonal timescales in the cold season. *Journal of Climate*, 36(22), 8027–8040. <https://doi.org/10.1175/JCLI-D-23-0155.1>
- Smedsrud, L. H., Esau, I., Ingvaldsen, R. B., Eldevik, T., Haugan, P. M., Li, C., et al. (2013). The role of the Barents Sea in the Arctic climate system. *Reviews of Geophysics*, 51(3), 415–449. <https://doi.org/10.1002/rog.20017>
- Sorokina, S. A., Li, C., Wettstein, J. J., & Kvamstø, N. G. (2016). Observed atmospheric coupling between Barents Sea Ice and the warm-Arctic cold-Siberian anomaly pattern. *Journal of Climate*, 29(2), 495–511. <https://doi.org/10.1175/JCLI-D-15-0046.1>
- Sorteberg, A., & Kvingedal, B. (2006). Atmospheric forcing on the Barents Sea winter ice extent. *Journal of Climate*, 19(19), 4772–4784. <https://doi.org/10.1175/JCLI3885.1>
- Stips, A., Macias, D., Coughlan, C., Garcia-Gorriz, E., & Liang, X. S. (2016). On the causal structure between CO₂ and global temperature. *Scientific Reports*, 6(1), 21691. <https://doi.org/10.1038/srep21691>
- Vannitsem, S., Dalaiden, Q., & Goosse, H. (2019). Testing for dynamical dependence: Application to the surface mass balance over Antarctica. *Geophysical Research Letters*, 46(21), 12125–12135. <https://doi.org/10.1029/2019GL084329>
- Vannitsem, S., & Ekemans, P. (2018). Causal dependences between the coupled ocean–atmosphere dynamics over the tropical Pacific, the North Pacific and the North Atlantic. *Earth System Dynamics*, 9(3), 1063–1083. <https://doi.org/10.5194/esd-9-1063-2018>
- Wilks, D. S. (2016). “The stippling shows statistically significant grid points”: How Research results are routinely overstated and overinterpreted, and what to do about it. *Bulletin of the American Meteorological Society*, 97(12), 2263–2273. <https://doi.org/10.1175/BAMS-D-15-00267.1>
- Woods, C., & Caballero, R. (2016). The role of moist intrusions in winter Arctic warming and Sea Ice decline. *Journal of Climate*, 29(12), 4473–4485. <https://doi.org/10.1175/JCLI-D-15-0773.1>

- Yashayaev, I., & Seidov, D. (2015). The role of the Atlantic Water in multidecadal ocean variability in the Nordic and Barents seas. *Progress in Oceanography*, 132, 68–127. <https://doi.org/10.1016/j.pocean.2014.11.009>
- Yeager, S. G., Karspeck, A. R., & Danabasoglu, G. (2015). Predicted slowdown in the rate of Atlantic sea ice loss. *Geophysical Research Letters*, 42(24), 10704–10713. <https://doi.org/10.1002/2015GL065364>
- Zhang, R. (2015). Mechanisms for low-frequency variability of summer Arctic sea ice extent. *Proceedings of the National Academy of Sciences*, 112(15), 4570–4575. <https://doi.org/10.1073/pnas.1422296112>
- Zheng, C., Ting, M., Wu, Y., Kurtz, N., Orbe, C., Alexander, P., et al. (2022). Turbulent heat flux, downward longwave radiation, and large-scale atmospheric circulation associated with wintertime Barents–Kara sea extreme Sea Ice loss events. *Journal of Climate*, 35(12), 3747–3765. <https://doi.org/10.1175/JCLI-D-21-0387.1>
- Zuo, H., Balmaseda, M. A., Tietsche, S., Mogensen, K., & Mayer, M. (2019). The ECMWF operational ensemble reanalysis–analysis system for ocean and sea ice: A description of the system and assessment. *Journal of Climate*, 15(3), 779–808. <https://doi.org/10.5194/os-15-779-2019>